

Fluorescence from atmospheric aerosol detected by a lidar indicates biogenic particles in the stratosphere

F. Immler¹, D. Engelbart², and O. Schrems¹

¹Alfred Wegener Institute for Polar and Marine Research, Am Handelshafen 12, 27570 Bremerhaven, Germany

²German Weather Service, Meteorological Observatory Lindenberg, Am Observatorium 12, 15848 Lindenberg, Germany

Received: 27 July 2004 – Accepted: 22 September 2004 – Published: 28 September 2004

Correspondence to: F. Immler (fimmiller@awi-bremerhaven.de)

5831

Abstract

With a lidar system that was installed in Lindenberg/Germany, we observed in June 2003, an extended aerosol layer at 13 km altitude in the lowermost stratosphere. This layer created an inelastic backscatter signal which we interpret as laser induced fluorescence from aerosol particles. Also, we find evidence for inelastic scattering in a smoke plume from a forest fire that we observed in the troposphere. Fluorescence from ambient aerosol had not yet been considered detectable by lidar. However, organic compounds such as polycyclic aromatic hydrocarbons sticking to the aerosol particles, or bioaerosol such as bacteria, spores or pollen fluoresce when excited with UV-radiation in a way that is detectable by our lidar system. Therefore, we conclude that fluorescence from organic material released by biomass burning creates the inelastic backscatter signal that we measured with our instrument and thus demonstrate a new and powerful way to characterize aerosols by a remote sensing technique. The stratospheric aerosol layer that we have observed in Lindenberg for three consecutive days is likely to be a remnant from Siberian forest fire plumes lifted across the tropopause and transported around the globe.

1 Introduction

Soot released by combustion into the atmosphere absorbs radiation and therefore heats the climate counteracting the cooling effect generally assigned to anthropogenic aerosols (Chung and Seinfeld, 2002). Aerosol particles are released either at the earth's surface from various sources, the crust (dust), the sea (sea salt aerosol) or by combustion processes (soot), or they form in situ by gas to particle conversion, like sulphate aerosol. While particles may enter the stratosphere in the tropics (Brock et al., 1995), the tropopause in the mid latitude efficiently suppresses tropospheric-stratospheric transport (TST)(Boering et al., 1994). However, recent observations of stratospheric aerosol layers by satellite-borne instruments and lidar suggest that strong

5832

thunderstorms are able to inject smoke from forest fires into the stratosphere at high latitudes (Fromm et al., 2000). Most recent in situ measurements also proof the presence of forest fire particles in the stratosphere (Jost et al., 2004). Even though these layers are optically thin, they are highly relevant because when aerosols leave the troposphere they escape their most efficient removal mechanism which is wet scavenging and consequently their lifetimes are strongly prolonged. The implications of particles in the stratosphere on the radiative balance and chemistry crucially depend on their physical and chemical properties. Ground or satellite based sensors are able to measure the distribution and optical depth of aerosols but usually provide little information on the exact type and source of the particles (Kaufman et al., 2002).

Lidar is a powerful tool to investigate into atmospheric aerosol since it allows to measure its distribution from near to the ground up to 30 km altitude and more with high vertical and temporal resolution. The different lidar techniques applicable to aerosol measurements like multi-wavelength lidar, depolarisation measurement and Raman techniques allow the determination of the particle's macro and microphysical properties to some extent. However, a precise and reliable characterization of aerosol based on lidar data which includes a description of its size distribution and chemical composition is generally hampered by the limited information available from this remote sensing techniques.

Here, we report the observation of a stratospheric aerosol layer by a ground based lidar system. This layer gave rise to a red shifted inelastic backscatter signal that we detected with our instrument and interpret as laser induced fluorescence created by the aerosol particles. We first briefly describe the methods used for this observations and the results obtained from them. We will then explain why we are confident that laser induced fluorescence is the only explanation for the optical features detected from that stratospheric layer and report on measurements from tropospheric layers that indicate that this optical behaviour is typical for forest fire smoke plumes.

5833

2 Method

The Mobile Aerosol Raman Lidar (MARL) of the Alfred Wegener Institute (AWI) was designed for measurements of aerosols and water vapour in the stratosphere and upper troposphere (Schäfer et al., 1995). It detects light backscattered by molecules and condensed matter in the atmosphere from outgoing laser beams at 532 nm and 355 nm. Inelastic Raman backscatter from nitrogen is detected at 387 nm and 607 nm and allows the direct retrieval of the aerosol extinction coefficient α (Ansmann et al., 1992). An additional detection channel at 407 nm with a bandwidth of 5.7 nm detects the vibrational Raman scattering from H₂O and allows the determination of the water vapour mixing ratio profiles up to about 8 to 10 km at night time according to a method first introduced by Melfi (1972). Radiosonde (Vaisala RS 80) data provided by the German weather service (DWD) from four daily launches at the site deliver a temperature and humidity profile and allow the determination of the tropopause height. They also served for calibrating the water vapour measurements of the lidar.

The emitter of the lidar is a Nd:YAG with frequency doubling and tripling, generating laser pulses with about 300 mJ at both 355 nm and 532 nm with a repetition rate of 30 Hz and a pulse duration of 8 ns. The receiver is based on a Cassegrain telescope with 1.1 m aperture coupled by two fibre bundles to the 10-channel polychromator. Our system is able to perform unattended measurements and can be controlled via the internet, thus enabling us to win a large dataset even with low manpower available. Unbroken data records spanning several consecutive days were achieved on occasions owing to the high grade of automation of the system.

Beside water vapour and cirrus clouds one main focus of our measurements is on tropospheric aerosol. It has been demonstrated on previous ship-borne campaigns that our system is able to detect and differentiate dust from marine particles in the troposphere (Immler and Schrems, 2003). This is possible due to the fact that the depolarisation and the colour indices are different for these two types of aerosol. The colour index expresses the wavelength dependence of the backscatter coefficient $\beta(\lambda)$

5834

and is calculated by the following expression:

$$C_I = -\log(\beta(532 \text{ nm})/\beta(355 \text{ nm})) / \log(355 \text{ nm}/532 \text{ nm}) \quad (1)$$

Urban and biomass burning aerosol have again different optical properties and can be discriminated from the unpolluted types just mentioned. However, since they both contain soot and therefore have a similar colour index (Wandinger et al., 2002), it is difficult to differentiate between urban and biomass burning aerosol on the basis of elastic backscatter lidar data.

3 Observations

From April to October of 2003 we performed measurements at the Meteorological Observatory in Lindenberg (52.2° N, 14.1° E) near Berlin/Germany with our Raman lidar. During this measurement campaign, strong layers of aerosol in the troposphere were frequently detected, and on several occasions we also observed layers of haze in the lower stratosphere. The most pronounced observation of this kind was made during the first days of June 2003, when a 0.4 to 1 km thick aerosol layer was dwelling at an altitude of about 13 km – about 1 km above the thermal tropopause – for more than 72 h. Figure 1 shows the backscatter ratio R at 532 nm as a function of time and altitude from 1 June 2003. R is the total atmospheric backscatter divided by the purely molecular contribution and thus a measure for the content of aerosol particles with 1 referring to a clear air. Between 4 and 8 km altitude aerosol some thin layers of aerosol are present, around 12 km some scattered cirrus clouds are marked by strong backscatter (R>5) above which a thin and steady layer emerges at about 12 km altitude. This layer persisted for the rest of the day, gaining altitude and staying at 13 km throughout 2 June and most of 3 June (Fig. 2).

The tropopause was at some times during this period split into a lower lapse rate tropopause (LPT) as defined by the standard WMO definition and the cold point tropopause (CPT). On the first day of the observation, 1 June 2003, LPT and CPT

5835

were at the same height, up to 1 km below the aerosol layer. This is demonstrated in Fig. 2 where the lapse rate tropopause and the cold point as determined from the radiosonde measurements are shown as solid and dashed lines, respectively. Around noon on 2 June 2003 the situation changed and a new temperature minimum appeared in 13.5 km altitude, just above the aerosol layer. The mean temperature in the aerosol layer itself decreased gradually from 213.5 to 209 K during the course of the three days (Fig. 3).

The layer at 13.5 km is clearly above the thermal tropopause but below 380 K potential temperature (Fig. 4) which marks the level where air can be introduced into the stratosphere exclusively in the tropics (Holton et al., 1995). Therefore we assign this aerosol layer to the lowermost stratosphere.

The stratospheric aerosol layer was 400–1000 m (650±300 m, mean ± std. dev.) thick and the backscatter ratio of the layer varied in the range from 1.5 to 4 at 532 nm. The optical depth at 532 nm determined from the nitrogen Raman signals varied from below 0.01 to 0.05 (0.026±0.013). Within the accuracy of our measurements the values at 355 nm were about the same (0.02±0.01). From these measurements the lidar ratio $S=\alpha/\beta$ can also be determined, yielding considerably high values of 86±30 sr for 355 nm and 100±20 sr for 532 nm. The colour index (C_I) of the layer is with 1.0±0.2 fairly constant throughout the whole period. The cloud shows a significant depolarisation with a clear diurnal cycle, reaching 20% during the day and dropping to 5% at night time (at 355 nm). Using scattering theory an estimate of the effective radius r_{eff} can be retrieved from the colour index. Depending on the refractive index that we assume we find values between 0.08 and 0.3 µm. The number concentration of the layers is calculated to be 500 to 2000 cm⁻³ (using $r_{eff}=0.1$ µm).

These optical properties suggest absorbing, solid material containing soot with effective radii in the order of 0.1 µm. These properties are typical for aged polluted aerosol from urban regions or from biomass burning (Wandinger et al., 2002) and different from typical optical properties of dust, sea salt or sulphate (Immler and Schrems, 2003). Finding aerosol of such properties in the lowermost stratosphere is an intriguing

5836

result, especially given the longevity of this layer, nevertheless there is one more very remarkable observation: Besides the backscatter ratio and temperature profiles, Fig. 3 shows the signal of the 407 nm channel of our instrument. On 1 June and 2 June, at night time (Fig. 3a and b, daytime measurements at 407 nm are not available) there is a clear peak at the altitude of the stratospheric aerosol layer at about 13 km. This statistically significant signal was present throughout both these nights, its strength correlated with the elastic backscatter signal of the aerosol layer.

With at least 10^9 , our system provides a sufficient suppression of the elastic backscatter in the 407 nm channel and therefore cross talk does not occur and has never been observed, even in the presence of low clouds that give rise to very strong elastic backscatter (Fig. 5). We have also never observed other unwanted effects in our Raman channel like after-pulsing or strong signal induced noise, that could explain the unusual signal at 13 km altitude (corresponding to a delay of $86 \mu\text{s}$ after the laser shoots). We therefore concluded that we detected inelastic scattering originating from the stratospheric aerosol layer, but it was not clear in the first place what could cause such a strong inelastic signal at that altitude.

4 Discussion

The first interpretation of this unusual feature was that there is a high water vapour content in that plume. However, this explanation can be ruled out since the relative humidity above ice according to the calibrated 407 nm signal would be up to several thousand percent given the low temperature at the corresponding altitude. Even though high super saturations have been observed in the atmosphere, such high values are not conceivable and definitely out of range, in particular in the presence of particles. Also, the radiosonde data does not indicate any enhancement of water vapour in that region (Fig. 4).

In the condensed phase, the Raman lines of H_2O are shifted towards smaller wavelengths (Slusher and Derr, 1975). We would therefore not expect interference from

5837

inelastic Raman scattering neither from ice nor from water (which is unlikely to exist at those temperatures). This is confirmed in Fig. 3c where the ice particles of the cirrus cloud at the tropopause, directly below the aerosol layer, do not create a detectable inelastic signal in the 407 nm channel, even though its elastic backscatter with a value of approximately 30 is by a factor of 10 higher compared to that of the aerosol layer above. This profile shows clearly, that neither cross talk from strong elastic backscatter, nor inelastic scattering from ice particles is measured by our system. We therefore came to the conclusion that the observed inelastic backscatter signal in the stratospheric aerosol plume is not caused by water, neither liquid nor solid nor in the gas phase.

4.1 Portuguese forest fire plumes

Usually, a comparison between the water vapour profiles measured with the 407 nm channel and data from a radiosonde launched at the same time are in accordance up to an altitude of about 8 to 10 km even in the presence of strong aerosol layers. This is demonstrated with a measurement made in Lindenberg on 16 September 2004, a day with strong aerosol content in the boundary layer and some cirrus clouds above (Fig. 5). The left plot of Fig. 5a shows the difference between the sonde data and the lidar results in blue on the same scale as used for plot of the measurements of the stratospheric layer in (Fig. 4b). The radiosonde data and lidar results are in good agreement throughout the whole lower and middle troposphere and are not significantly biased by the presence of clouds or aerosol.

However, we found a significant discrepancy between sonde and lidar during a number of consecutive days in early August 2003, when the water vapour mixing ratio retrieved from the lidar data showed a systematic deviation from the moisture measurements of the radiosonde. A fairly strong layer of aerosol was present in these measurements throughout the troposphere with backscatter ratios up to 3 (Fig. 6). During this period heavy forest fires were reported in Portugal. The backward trajectories shown in Fig. 7 give a clear indication, that the aerosol we detected in Lindenberg were smoke plumes from these forest fires. Figure 6 shows on the right side the differ-

5838

ence detected between the water vapour mixing ratio retrieved from the lidar data and those from the radiosonde. The errorbars indicate the total error and show that there is a significant positive bias in the lidar data.

This bias correlates with the concentration of smoke aerosol that is displayed in green in terms of the elastic backscatter signal measured with the lidar. This correlation suggests, that the aerosol particles itself create the bias by inelastic scattering. The most likely explanation for this finding is laser induced fluorescence on aerosol particles.

4.2 Fluorescence lidar

There is a long tradition of using laser induced fluorescence for remote sensing of the atmosphere. Hydroxyl (OH) and metal atoms such as sodium, potassium or iron have been detected by resonant fluorescence in the mesosphere in 85 km altitude and allow the determination of the temperature and wind at these altitudes (Brinksma et al., 1998; Neuber et al., 1988; von Zahn and Höffner, 1996). In the lower troposphere however, fluorescence by atoms or molecules in the gas phase is severely hampered by collisional quenching of the excited states due to the high pressure. On the other hand fluorescence of mainly organic substances still allow interesting applications near or at the earth's surface. For instance, contamination of soils with petroleum products is detected in situ with high sensitivity using fluorescence (Schultze et al., 2004) and fluorescence lidars are used for detecting oil spills, phytoplankton and chlorophyll in the ocean (Cecchi et al., 2003).

The investigation of fluorescence from polycyclic aromatic hydrocarbons adsorbed on suspended particles was pioneered by Allegrini and Omenetto (1979) and Niessner et al. (1991). The fluorescence spectra of Benzo[a]pyrene (BaP, C₂₀H₁₂) in water for example, shows a wide band covering the 407 nm region when excited at 355 nm (Fernández-Sánchez et al., 2003) and therefore could in principal be detected with the set-up used by our lidar. BaP is an ubiquitous product of incomplete combustion and stable in the atmosphere. BaP and others PAHs adsorbed on soot in a smoke plume

5839

are known to persist for many days in the atmosphere (Behymer and Hites, 1988). In polluted air BaP was found in amounts of 200 pg m⁻³ (Schauer et al., 2004). The presence of BaP and other PAHs in cigarette smoke is not only one of the reasons for the carcinogenic effect of smoking, they are also the cause for the fluorescence exhibited by the smoke of tobacco leaves (Hill et al., 1999). A similar fluorescence spectrum such as the one from BaP was measured from bacteria and fungal spores (Hill et al., 1999). The detection and discrimination of biological particles in the atmosphere by their intrinsic fluorescence has received greater recognition in the recent years (Hairston et al., 1997). Besides in-situ detection, the remote detection of disseminated spores by a fluorescence lidar up to a distances of several kilometers have been reported (Christesen et al., 2004).

Biogenic aerosols obviously have the potential to fluoresce at atmospheric conditions when excited with a laser beam like the one used in our lidar, due to the fact that they contain PAH as well as spores and pollen. To estimate the sensitivity of our instrument regarding the detection of fluorescence, we calculated the backscatter coefficient at 407 nm within the stratospheric aerosol layer. To do this, the signal needs to be calibrated. This can easily be done using radiosonde data as a calibration standard at low altitudes, in a region where interference from fluorescence is certainly negligible. This calibration delivers the water vapour mixing ratio profile $WVMR(h)$ from which the concentration profile $C_{WV}(h)$ can be calculated using atmospheric density profile which can be derived from the radiosondes temperature and pressure measurements. The result is shown in Fig. 4b. The backscatter coefficient measured with 407 nm channel, β_{WV} is then

$$\beta_{WV}(h) = C_{WV}(h) \times \sigma_{WV} \quad (2)$$

using the known scattering cross section σ_{WV} of the H₂O Raman line at 3599 cm⁻¹ which is 6 × 10⁻³⁰ cm² sr⁻¹ (Turner and Whiteman, 2002). Accordingly, the peak at 13 km (Fig. 4b) corresponds to a backscatter coefficient in the order of 10⁻¹³ cm⁻¹ sr⁻¹. This is six orders of magnitude lower than the elastic backscattering coefficient of the

5840

aerosol and about two orders lower than the Raman backscatter coefficient of nitrogen at that altitude.

Unfortunately, little is reported about the cross sections of fluorophores like PAH on aerosol particles. Also, the efficiency of such a process in the atmosphere depends on many parameters including temperature and pressure hampering an assessment of the possibility of detecting the fluorescence from these agents by our lidar. However, measurements of cross sections of the fluorescence of bacteria and pollen are available, a value of $5 \times 10^{-14} \text{ cm}^2 \text{ nm}^{-1} \text{ particle}^{-1}$ for *Bacillus globigii* (Bg) and $2 \times 10^{-13} \text{ cm}^2 \text{ nm}^{-1} \text{ particle}^{-1}$ for pine pollen when excited with light at 230 nm are reported by Stephens (1999). Given a scattering cross section in this order of magnitude, a concentration of fluorescing particles of about 0.1 cm^{-3} is needed to explain the measured signal. Given the concentration of particles estimated from the elastic backscatter which was about $1,000 \text{ cm}^{-3}$ this means that one out of 10^4 particles in the plume should fluoresce in order to explain the inelastic signal that we have measured.

The concentration of bacteria in ambient air is 0.001 to 0.01 cm^{-3} (Ariya and Amyot, 2003) and slightly below our limit of detection. An enhancement of bioparticles that may fluoresce is likely to occur in the plume of a forest fire. However, the concentration of this kind of particles might still be too low to be detected by our system. This suggests that PAH on soot is the more important agent and creates most of the observed fluorescence in the aerosol.

These rough estimates demonstrate that it is realistic to assume that a sensitive instrument like ours is able to detect the fluorescence of pyro-biogenic particles in an elevated smoke plume. The powerful laser, the large receiving telescope (1.1 m), and the large bandwidth (5.7 nm) and good performance of the 407 nm channel makes our system particularly suitable for discovering laser induced fluorescence on particles in the atmosphere.

5841

5 Conclusions

By a thorough examination of the data obtained in Lindenberg, we come to the conclusion that we have detected laser induced fluorescence from aerosol particles in the troposphere and the lowermost stratosphere. The detection of a fluorescence signal from atmospheric aerosol has not yet been reported anywhere in literature. However, the results presented above demonstrate that it is definitely conceivable, that the aerosol layer we have detected at 13 km altitude for three days contains fluorescing material from biomass burning. We can rule out that cross talk from elastic scattering or Raman scattering from water in any phase has created the inelastic signal that we have measured at 407 nm.

The fact that the elastic optical properties of this aerosol are those of an aerosol containing soot supports the hypothesis of a forest fire plume in the stratosphere. Moreover, at that particular time, spring 2003, forest fires were abundant across the northern hemisphere, including an unprecedented 21 million hectares of boreal forest burned in Siberia (Fromm et al., 2004). Backward trajectories trace the air mass that we observed on 02/06/2003 in Lindenberg back to the Pacific region where it obviously experienced convection (Fig. 8). Fromm et al. (2000) have suggested that extreme convection triggered by forest fires may be able to inject aerosol into the stratosphere at high latitudes. These convective regions in the Pacific (Fig. 8) are detached from potential continental sources of the aerosol in Siberia and therefore do not support the idea of a direct injection of the forest fire smoke from thunderstorms created by the fires themselves. At that particular time a tropical storm, the Typhoon Chan Hom was active in that region and might have created a TST event that included polluted air from Asia.

In the first few hours of our observation the aerosol layer was not clearly separated from the cirrus clouds in the layer below (Fig. 1). This observation and the subsequent rising motion of the layer suggest another transport mechanism: slow updraft by radiative heating could also play a role in bringing the material from the upper troposphere

5842

into the stratosphere. According to the trajectories (Fig. 8) the upper tropospheric air-mass has been traveling at its level for about a week or more. The back-trajectory calculation does not deliver reliable results for such long time periods. It is therefore difficult and beyond the scope of this work to determine whether convective transport, isentropic flow from the subtropics or radiative ascent is the dominating process to convey the biogenic aerosol into the lowermost stratosphere.

The dynamical processes remain to be investigated in detail, and the same holds for the exact particle types and chemical compounds that create the fluorescence of atmospheric aerosol which we have measured. Nevertheless, as we have demonstrated, there is the possibility of using fluorescence for remote sensing of aerosol in the UTLS region. This unprecedented finding opens up new opportunities for remote sensing of the distribution and the composition of particles from sources such as forest fires and fossil fuel burning and could therefore overcome some of the shortcomings of current techniques. These data are important prerequisites to assess the climatic impact of these types of anthropogenic aerosol, which is currently still debated (IPCC, 2001; Jacobson, 2001; Feichter et al., 2003). Lidar techniques based on fluorescence detection could become a powerful tool to study the abundance of such aerosol as well as exchange processes between the upper troposphere and the lower stratosphere. Our observation of an aerosol layer lasting for three days above the tropopause, shows an interesting, rarely detected example of such an event in the tropopause region.

Acknowledgements. We like to thank the British Atmospheric data centre for providing access to ECMWF data and performing trajectory calculations. Thanks to I. Beninga, W. Ruhe (impres GmbH) and the staff at MOL for assisting the experiments, to D. Kaiser and A. Schulz for supportive discussions.

References

- Allegrini, I. and Omenetto, N.: Laser-induced fluorescence and raman scattering for real time measurement of suspended particulate matter, *Environ. Sci. Tech.*, 13, 3, 349–350, 1979. 5843
- 5839
- Ansmann, A., Wandinger, U., Riesbel, M., Weitkamp, C., and Michaelis, W.: Independent measurement of extinction and backscatter profiles in cirrus clouds by using a combined raman elastic-backscatter lidar, *Appl. Opt.*, 31, 7113–7131, 1992. 5834
- Ariya, P. and Amyot, M.: The role of bioaerosols in atmospheric chemistry and physics, *Atmos. Environ.*, 38, 1231–1232, 2003. 5841
- Behymer, T. and Hites, R.: Photolysis of polycyclic aromatic hydrocarbons adsorbed on fly ash, *Environ. Sci. Tech.*, 22, 11, 1311–1319, 1988. 5840
- Boering, K. A., Daube, B. C. J., Wofsy, S. C., Loewenstein, M., Podolske, J. R., and Keim, E. R.: Tracer-tracer relationships and lower stratospheric dynamics: CO₂ and N₂O correlations during spade (CO₂, N₂O), *Geophys. Res. Lett.*, 21, 2567–2570, 1994. 5832
- Brinksma, E. J., Meijer, Y. J., McDermid, I. S., Cageao, R. P., Bergwerff, J. B., Swart, D. P. J., Ubachs, W., Matthews, W. A., Hogervorst, W., and Hovenier, J. W.: First lidar observations of mesospheric hydroxyl, *Geophys. Res. Lett.*, 25, 51–54, 1998. 5839
- Brock, C. A., Hamill, P., Wilson, J. C., Jonsson, H. H., and Chan, K. R.: Particle formation in the upper tropical troposphere: A source of nuclei for the stratospheric aerosol, *Science*, 270, 1650–1653, 1995. 5832
- Cecchi, G., Lognoli, D., and Mochi, I.: Fluorescence lidars and their potentials for the remote sensing of the marine environment, *Elsevier oceanography series*, 69, 71–77, 2003. 5839
- Christesen, S., Merrow, C., DeSha, M., Wong, A., Wilson, M., and Butler, J.: Uv fluorescence lidar detection of bioaerosols, *SPIE*, Vol. 2222, 228–237, 2004. 5840
- Chung, S. and Seinfeld, J.: Global distribution and climate forcing of carbonaceous aerosols, *J. Geophys. Res.*, 107, 4407, 2002. 5832
- Feichter, J., Sausen, R., Graßl, H., and Fiebig, M.: Comment on “control of fossil fuel particulate black carbon and organic matter, possibly the most effective method of slowing global warming”, *J. Geophys. Res.*, 108, 4767, 2003. 5843
- Fernández-Sánchez, J., Segura-Carretero, A., Costa-Fernández, J. M., Bordel, N., Pereiro, R., Cruces-Blanco, C., Sanz-Medel, A., and Fernández-Gutiérrez, A.: Fluorescence optosensors based on different transducers for the determination of polycyclic aromatic hydrocarbons in water, *Anal. Bioanal. Chem.*, 377, 4, 614–623, 2003. 5839
- Fromm, M., Alfred, J., Hoppel, K., Hornstein, J., Bevilacqua, R., Shettle, E., Servranckx, R., Li, Z., and Stocks, B.: Observations of boreal forest fire smoke in the stratosphere by POAM III, SAGE II, and lidar in 1998, *Geophys. Res. Lett.*, 27, 1407, 2000. 5833, 5842

- Fromm, M., Bevilacqua, R., Stocks, B., and Servranckx, R.: New directions: Eruptive transport to the stratosphere: Add fire-convection to volcanoes, *Atmos. Environ.*, 38, 163–165, 2004. [5842](#)
- Hairston, P., Ho, J., and Quant, F.: Design of an instrument for real-time detection of bioaerosols using simultaneous measurement of particle aerodynamic size and intrinsic fluorescence, p. 471–482, *J. Aeros. Sci.*, 28, 3, 345–538, 1997. [5840](#)
- Hill, S. C., Pinnick, R. G., Niles, S., Pan, Y.-L., Holler, S., Chang, R. K., Bottiger, J., Chen, B., Orr, C.-S., and Feather, G.: Real-time measurement of fluorescence spectra from single airborne biological particles, *Field A.C.T.*, 3, 4–5, 221–239, 1999. [5840](#)
- Holton, J. R., Haynes, P. H., McIntyre, M. E., Rood, R. B., Douglass, A. D., and Pfister, L.: Stratosphere-troposphere exchange, *Rev. Geophys.*, 33, 4, 403–439, 1995. [5836](#)
- Immler, F. and Schrems, O.: Vertical profiles, optical and microphysical properties of Saharan dust layers determined by a ship-borne lidar, *Atmos. Chem. Phys.*, 3, 1353–1364, 2003, SRef-ID: [1680-7324/acp/2003-3-1353](#). [5834](#), [5836](#)
- IPCC: Third Assessment report – Climate Change, Cambridge University press, 2001. [5843](#)
- Jacobson, M.: Strong radiative heating due to the mixing state of black carbon in atmospheric aerosols, *Nature*, 409, 695–697, 2001. [5843](#)
- Jost, H.-J., Drdla, K., Stohl, A., Pfister, L., Loewenstein, M., Lopez, J. P., Hudson, P. K., Murphy, D. M., Cziczo, D. J., Fromm, M., Bui, T. P., Dean-Day, J., Gerbig, C., Mahoney, M. J., Richard, E. C., Spichtinger, N., Pittman, J. V., Weinstock, E. M., Wilson, J. C., and Xueref, I.: In-situ observations of mid-latitude forest fire plumes deep in the stratosphere, *Geophys. Res. Lett.*, 31, L11 101, 2004. [5833](#)
- Kaufman, Y. J., Haywood, J. M., Hobbs, P. V., Hart, W., Kleidman, R., and Schmid, B.: Remote sensing of vertical distributions of smoke aerosol off the coast of africa, *Geophys. Res. Lett.*, 29, 1831–1834, 2002. [5833](#)
- Melfi, S.: Remote measurements of the atmosphere using raman scattering, *Appl. Opt.*, 11, 1605–1610, 1972. [5834](#)
- Neuber, R., von der Gathen, P., and von Zahn, U.: Altitude and temperature of the mesopause at 69°N latitude in winter, *J. Geophys. Res.*, 93, 11 093–11 101, 1988. [5839](#)
- Niessner, R., Robers, W., and Krupp, A.: Detection of particulate polycyclic aromatic hydrocarbons by laser-induced time-resolved fluorescence, *Fresenius J. Anal. Chem.*, 341, 207–213, 1991. [5839](#)
- Schäfer, H.-J., Schrems, O., Beyerle, G., Hofer, B., Mildner, W., Theopold, F., Lahmann, W.,

5845

- Weitkamp, C., and Steinbach, M.: A modular and mobile, multi-purpose lidar system for observation of tropospheric and stratospheric aerosols, *SPIE EurOpto Series* 2581, 128–136, 1995. [5834](#)
- Schauer, C., Niessner, R., and Pöschl, U.: Analysis of nitrated polyaromatic hydrocarbons by liquid chromatography with fluorescence and mass spectrometry detection: air particulate matter, soot and reaction product studies, *Anal. Bioanal. Chem.*, 378, 725–736, 2004. [5840](#)
- Schultze, R., Lemke, M., and Löhmannsröben, H.-G.: Laser-induced fluorescence (lif) spectroscopy for the in situ analysis of petroleum product-contaminated soils, in *Laser in environmental and life science*, edited by Hering, P., Lay, J. P., and Stry, S., Springer, 79–98, 2004. [5839](#)
- Slusher, R. and Derr, V.: Temperature dependence and cross section of some stokes and anti-stokes raman lines in ice Ih, *Appl. Opt.*, 14, 2116–2120, 1975. [5837](#)
- Stephens, J.: Measurements of the ultraviolet fluorescence cross sections and spectra of bacillus anthracis simulants, Final report, LOS ALAMOS NATIONAL LAB NM, 48, 1999. [5841](#)
- Turner, D. D. and Whiteman, D.: Remote Raman spectroscopy, profiling water vapor and aerosols in the troposphere using raman lidars, *Handbook of vibrational spectroscopy*, 2002. [5840](#)
- von Zahn, U. and Höffner, J.: Mesopause temperature profiling by potassium lidar, *Geophys. Res. Lett.*, 23, 141–144, 1996. [5839](#)
- Wandinger, U., Müller, D., Böckmann, C., Althausen, D., Matthias, V., Bösenberg, J., Weiss, V., Fiebig, M., Wendisch, M., Stohl, A., and Ansmann, A.: Optical and microphysical characterization of biomass-burning and industrial-pollution aerosols from multiwavelength lidar and aircraft measurements, *J. Geophys. Res.*, 107, 8125, 2002. [5835](#), [5836](#)

5846

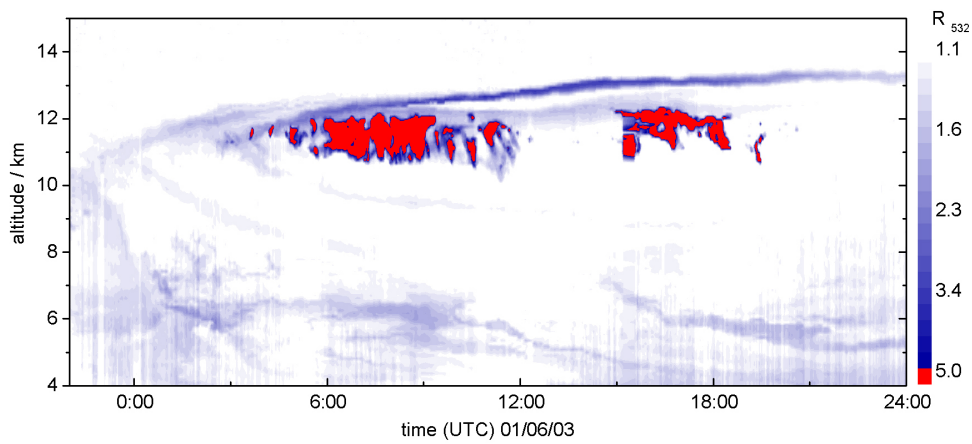


Fig. 1. Lidar backscatter ratio as a function of time and altitude from Lindenberg on 1 June 2003. Besides aerosol layers in the middle troposphere and cirrus clouds in around 12 km, a thin layer of particles in the lowermost stratosphere with a backscatter ration of about 3–4 was detected.

5847

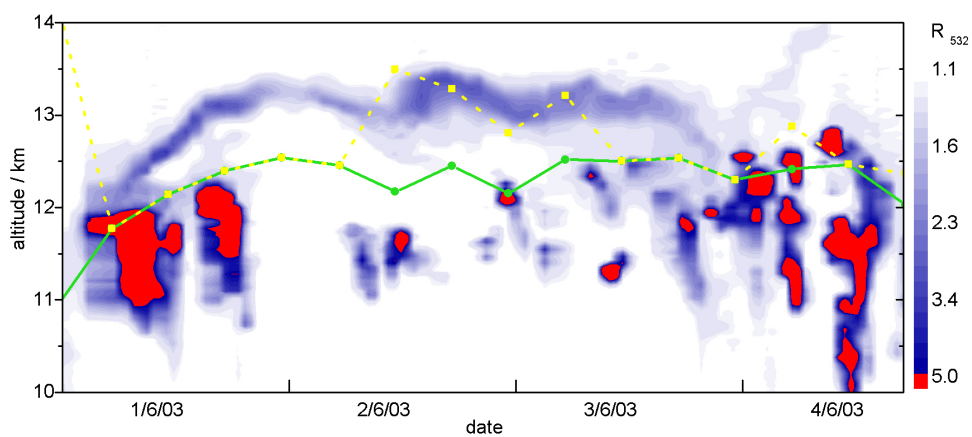


Fig. 2. Time-altitude plot of lidar backscatter ratio profiles measured in Lindenberg/Germany starting on 1 June 2003 00:00 UT and ending on 4 June 2003 17:00 UT. The solid line indicates the altitude of the lapse rate tropopause determined from radiosonde launches four times a day. The dashed line indicates the temperature minimum. Clouds appear in red due to their large backscatter.

5848

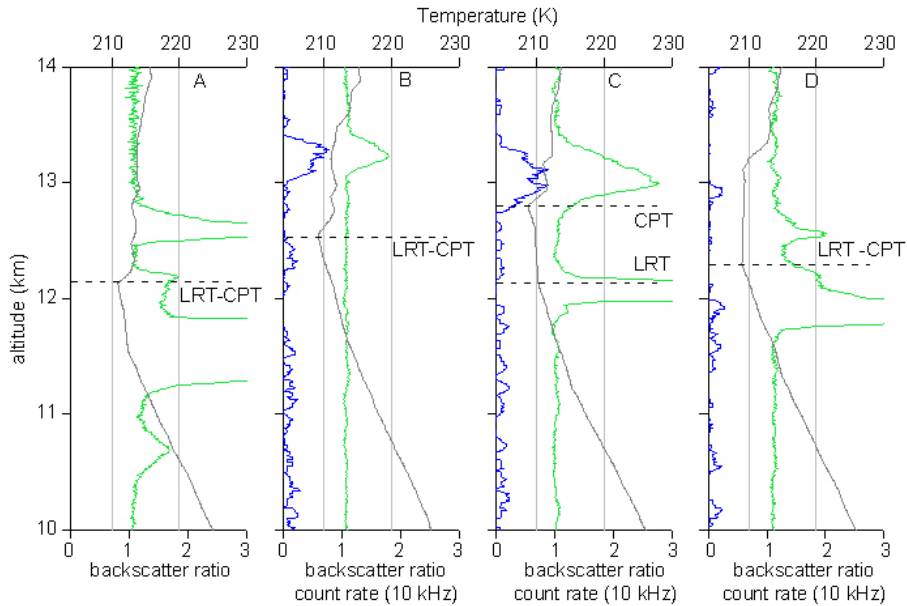


Fig. 3. Backscatter ratio profiles (green) measured on 1 June 2003 11:00 UT (start time, **A**), 22:12 (**B**), 2 June 2003 22:22 (**C**) and 3 June 2003 21:31 (**D**) in Lindenberg by the lidar (40 000 shots – 24 min mean). The temperature profiles measured at about the same time ($\delta t < 60$ min) by a radiosonde is shown in black lines. The dashed horizontal lines indicate the lapse rate (LRT) and the cold point tropopause (CPT). The blue curves show the signal detected in the 407 nm channel. It gives a clear response from the aerosol layer in 13 km altitude, but not from the cirrus clouds at about 12 km in C and D.

5849

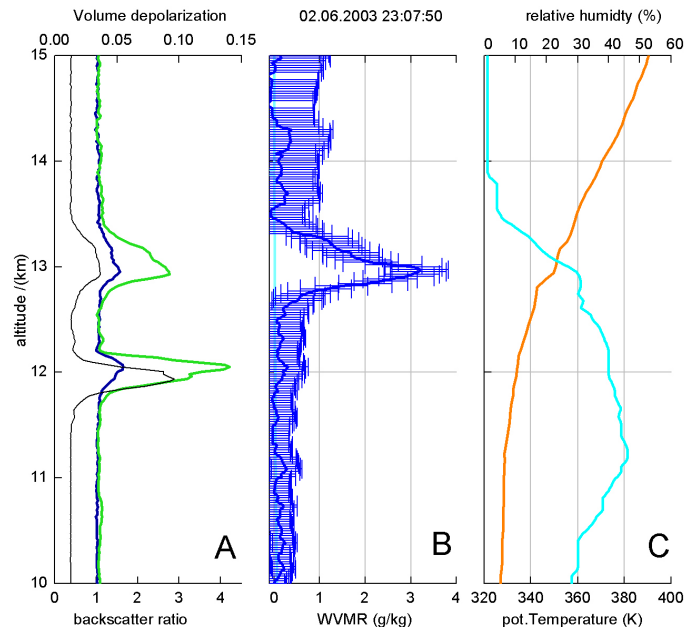


Fig. 4. Profiles from Lidar and radiosonde measurement from 2 June 2003 averaged from 22:44 to 23:07 UT. A radiosonde was launched at 22:45 UT and reached 13 km altitude at about 23:05 UT. The left plot shows the backscatter ratio at 532 nm (green) and 355 nm (blue). The black line indicates the Volume depolarisation. The plot in the middle displays the water vapour mixing ratio (WVMR) as determined by the calibrated lidar (dark green) and the radiosonde (cyan). At the right plot the relative humidity and the potential temperature from the radiosonde data is shown. The aerosol layer in the stratosphere at 13 km shows enhanced backscatter which can not be due to water vapour, since such high values up to 3 g/kg are unrealistic in the lowermost stratosphere. The bars show the total error derived from Poisson statistics and potential systematic errors.

5850

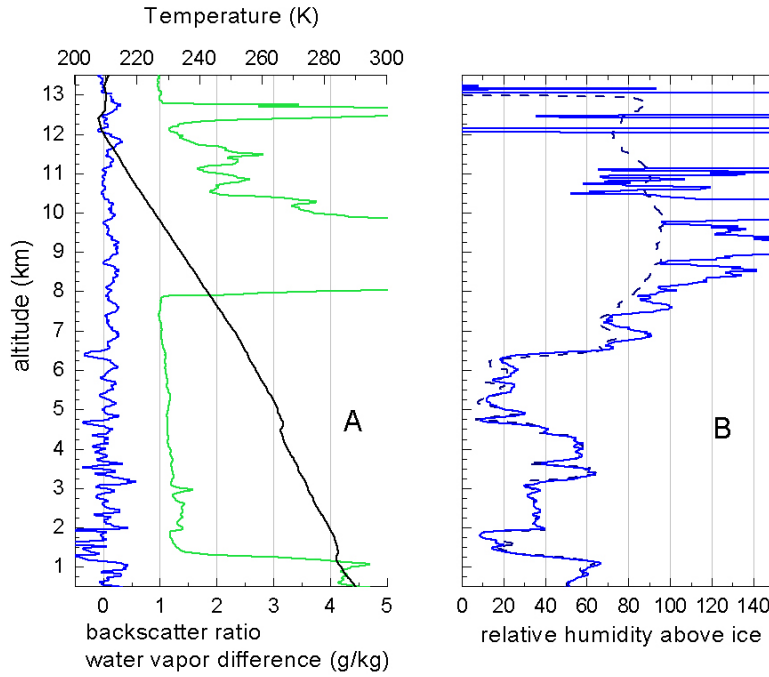


Fig. 5. Water vapour measurements by Raman lidar and Radiosonde from 16 June 2003 in Lindenberg. The plot at the right shows the relative humidity above ice retrieved from the inelastic lidar data (solid blue) and detected by the radiosonde (dashed). The Lidar data is integrated between 22:36 and 23:00 (60 000 shots), the radiosonde was launched at 22:45 UTC. The left plot shows the differences of both measurements in units of g/kg (blue) along with the elastic backscatter ratio (green) and the temperature (black). Both measurements show good agreement also in the presence of strong aerosol in the boundary layer and in the presence of clouds above 8 km.

5851

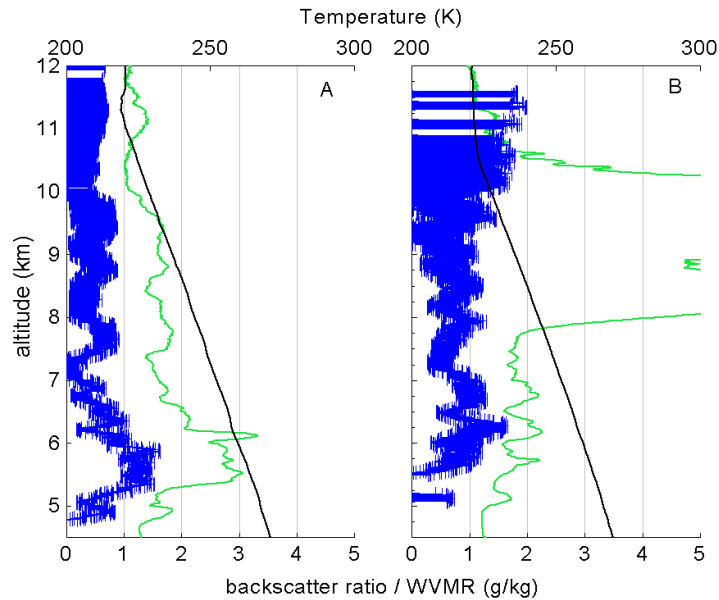


Fig. 6. Biomass burning aerosol detected above Lindenberg on 5 August 2003. The green curve shows the backscatter ratio at 532 nm with the plume between 5.0 and 10 km indicated by backscatter ratios between 1.2 and 3.5. The black curves shows the temperature. The blue curves show the water vapour mixing ratio retrieved from the 407 nm Raman channel minus that measured by a radiosonde at the same time. The excess signal in the water vapour measured by the lidar correlates with the backscatter profile and is therefore attributed to fluorescence. The right panel shows the same profiles some hours later when a cloud was present in the upper part of the aerosol layer. Obviously the aerosol layer accounts for the deviation found in the water vapour profile while the cirrus cloud in the upper part of the layer, marked by backscatter ratios greater than 5, does not.

5852

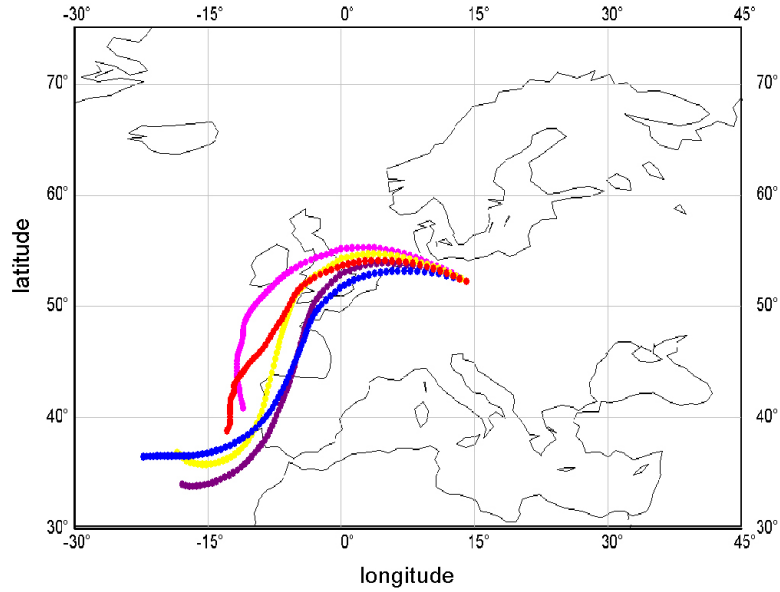


Fig. 7. Backward trajectories for Lindenberg, 5 August 2003, 18:00 UTC at about which time the measurement of Fig. 6 was made. The trajectories lead back to Portugal, from where at that time strong activity from forest fires were reported.

5853

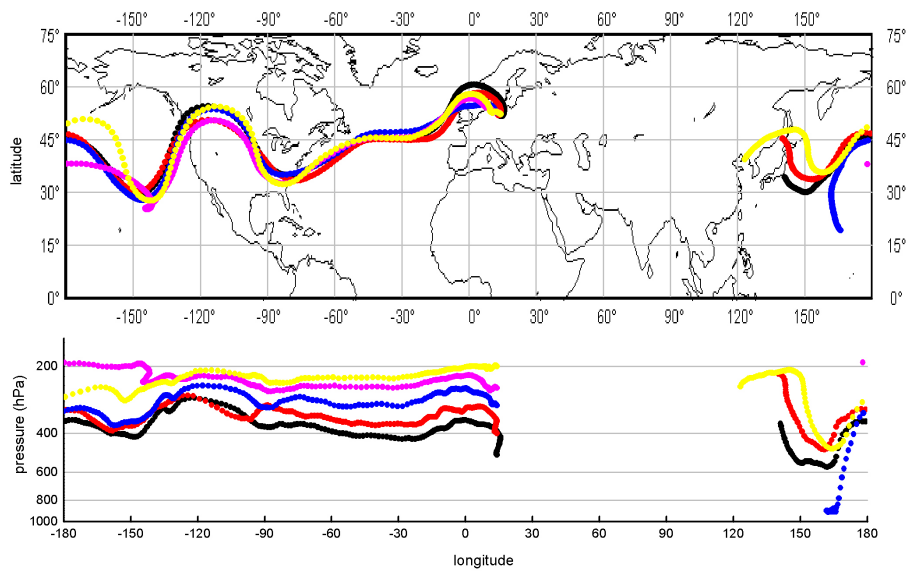


Fig. 8. Backward trajectories calculated for 2 June, 00:00 UT, when the stratospheric aerosol was detected in 13 km altitude (Fig. 2). The corresponding trajectory (yellow) traced back for 10 day ends in the northern Pacific region where at that time a typhoon was active.

5854